Computer Networks 254 (2024) 110733

Contents lists available at ScienceDirect

Computer Networks

journal homepage: www.elsevier.com/locate/comnet

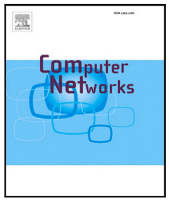

An energy-efficient JT-CoMP enabled framework with adaptive OMA/NOMA in HetNets

Aamina Akbar [a,b], Ashfaq Ahmed [c], Adnan Zafar [a], Sobia Jangsher [d,*]

[a] Wireless and Signal Processing (WiSP) Lab, Institute of Space Technology (IST), Islamabad, Pakistan
[b] Department of Electrical and Computer Engineering, Foundation University School of Science and Technology (FUSST), Islamabad, Pakistan
[c] Department of Computer & Communication Engineering, Khalifa University, Abu Dhabi, 127788, United Arab Emirates
[d] School of Electronic Engineering, Dublin City University, Dublin, Ireland

ARTICLE INFO

Keywords:
Coordinated multi-point (CoMP)
Heterogeneous network (HetNet)
Non-orthogonal multiple access (NOMA)
Successive interference cancellation (SIC)
Hybid multiple-access
Energy efficiency (EE)

ABSTRACT

The increasing demand for higher data rates and improved energy efficiency (EE) in next-generation wireless networks necessitates the optimized selection of multiple-access and coordination techniques. A hybrid joint transmission (JT)-coordinated multi-point (CoMP) enabled orthogonal multiple access (OMA)/non-orthogonal multiple access (NOMA) technique, combining the spectral efficiency (SE) and capacity benefits of CoMP NOMA with the interference mitigation of CoMP OMA, offers a highly adaptable solution for future wireless networks. This paper studies the joint optimization of CoMP/non-CoMP selection, OMA/NOMA selection, power allocation, and user pairing, with the objective of maximizing the EE in the network. A Dynamic CoMP user selection with energy-efficient adaptive multiple access (DCEAMA) algorithm to solve the formulated problem is proposed. Our Monte Carlo simulations show that the DCEAMA surpasses both the pure CoMP OMA and CoMP NOMA schemes in terms of EE, with an average increase of 38% and 26% respectively. We compare our heuristic technique to an exhaustive search strategy to evaluate its efficiency. The findings indicate that our strategy produces comparable EE across various power levels with reduced computational complexity.

1. Introduction

The rapid expansion of the Internet of things (IoT) is creating a significant influx of data, fueled by a wide range of devices that vary from low-data rate sensor nodes to immersive smart home and transportation applications [1–3]. Nevertheless, this revolution encounters certain crucial obstacles: energy efficiency (EE), spectral efficiency (SE), high capacity and coverage at the cell edges. Sensor networks, which serve as the foundation of the IoT, continuously monitor environmental parameters such as heat, light, humidity, visibility, temperature, pressure, and vibrations. However, their crucial function depletes their batteries, often necessitating inconvenient replacements. Innovative and promising solutions by integrating several cutting-edge wireless technologies are needed to improve the lifetime, capacity, SE, ubiquitous connectivity, high reliability, and reduced latency of these critical devices to overcome these hurdles and unlock the full potential of 5G and beyond 5G (B5G) systems. The roll-out of fifth generation (5G) and research towards sixth generation (6G) in industry and academia have both resulted in influencing new capabilities and addressing the increasing demand for mobile data traffic [4,5].

Heterogeneous networks (HetNets) can enhance cell edge user performance and increase attainable rates. Small base station (SBS) deployment improves network capacity, SE, and coverage, but restricts network throughput owing to inter-channel interference (ICI). Given the limitations of signal processing techniques, it is necessary to explore alternative methods for managing ICI. By utilizing coordinated multi-point (CoMP), performance can be significantly enhanced through the coordination of transmitted signals from multiple cells to prevent mutual interference. The CoMP transmission mitigates the interference by coordinating the joint transmission from SBSs, resulting in improved received signal to interference plus noise ratio (SINR) and data rate for users which leads to a decrease in outages. Non-coherent joint transmission (JT) scheme is an advanced CoMP transmission method that enables sharing of data and control information between coordinating base stations (BSs) without phase-mismatch correction or strict synchronization [6]. While CoMP approaches have demonstrated an improvement in overall network performance, particularly for cell-edge users, they may also degrade network spectrum efficiency and waste valuable spectrum resources by limiting the number of users that can

* Corresponding author.
E-mail address: sobia.jangsher@dcu.ie (S. Jangsher).

https://doi.org/10.1016/j.comnet.2024.110733
Received 5 March 2024; Received in revised form 2 July 2024; Accepted 19 August 2024
Available online 22 August 2024

use the network. This is due to the fact that in CoMP transmission, several BSs that use orthogonal multiple access (OMA) coordinate to send data utilizing various resource blocks (RBs) to the same cell-edge user. The advantage of less inter-user interference and easier receiver designs comes at the cost of a restricted number of users who can use the spectrum [7].

In third generation partnership project (3GPP) long term evolution (LTE) Release 15, non-orthogonal multiple access (NOMA) is suggested as a viable B5G spectral-efficient solution to address the problem of OMA's spectral inefficiency. Power domain-NOMA enables high connectivity while maintaining user fairness and managing high traffic volumes [8–15]. To improve overall system throughput, users with different channel conditions are multiplexed within the same RB (time/frequency/code), allocating more power to distant users with poor channel conditions and less power to nearby users with good channel conditions. The primary motivation for applying NOMA in future communication systems is its capacity to accommodate many users rather than its SE. While NOMA can enhance SE, this benefit diminishes when users have comparable channel gains [15]. Nevertheless, it is unlikely that NOMA will fully replace OMA in future wireless networks, as there are various implementation challenges associated with NOMA beyond infrastructure demands [10]. In order for optimal performance, it is important to consider several factors. These include distinct channel gain difference among paired users, the complexity of the successive interference cancellation (SIC) receiver, potential delays and error propagation as the number of paired users increase, the presence of unpaired users, the power consumption associated with SIC processing, and the interference experienced by users at the edge of the cell. Even though NOMA uses the spectrum efficiently, its performance degrades or fails due to increased interference when there is a high user density or when the channel gain difference between the paired users is not distinct enough. Consequently, using a hybrid approach that incorporates both NOMA and OMA becomes desirable. It makes it possible to switch between these strategies dynamically, improving system performance in response to real-time channel conditions.

To meet the demands of a large number of IoT and mobile devices in B5G/6G, a dense deployment of SBSs is necessary. This impacts the EE of the network. Although CoMP helps address EE issues by managing interference and enhancing throughput, there is still potential to enhance EE by leveraging the adaptability of dynamic resource allocation. Typically, the goal is to maximize resources like SE, achievable rate, and quality of service (QoS). However, when discussing green communication, it is important to explore additional factors such as EE optimization. Energy-efficient ultra-dense networks can satisfy the needs of next-generation wireless communication systems by utilizing energy-efficient resource allocation algorithms to reduce power consumption overall. In this paper, we study the non-coherent JT-CoMP enabled hybrid OMA/NOMA framework that provides an energy-efficient solution for edge users in HetNets.

1.1. Related work

In multi-cell downlink NOMA, the interference from neighboring cells is more significant for edge users than it is from their own cells [15]. However, in uplink NOMA, the interference received at the BS is directly related to the number of users in each NOMA user pair of the neighboring cells. Given that the interference is received at the BS, which serves as a centralized entity, all users within a specific NOMA cluster will experience it equally [8]. An uplink CoMP transmission technique called network NOMA is proposed in [16] to enhance system throughput and SE. Several CoMP NOMA techniques have been examined in [7], with a focus on JT-CoMP NOMA, to prevent ICI in a downlink multi-cell NOMA system. For every coordinating cell, a low-complexity distributed optimal power allocation technique is suggested.

In [17,18], authors use a dynamic power allocation method to maximize EE while taking into account users' QoS and maximum BS transmit power constraints. The optimization issue in [17] is non-convex; hence, an iterative, sub-optimal, rapid converging, and low complexity solution that combines fractional programming and difference of convex programming is proposed to solve it. Nevertheless, [18] analyzes the resource allocation problem with imperfect SIC and channel state information (CSI) conditions, taking into account power allocation and user scheduling for maximizing EE. Authors in [19–21] discuss a generalized CoMP NOMA system where JT-CoMP is applied to all cell center and cell edge users. A low complexity clustering algorithm that uses an optimal power allocation strategy for every cluster is investigated in [19].

The performance of cell edge users deteriorates due to ICI in multi-cell settings and an increase in the number of low-powered SBSs that are positioned closely. The introduction of CoMP in NOMA HetNets aims to improve SINR of cell edge users and mitigate ICI, thereby improving the performance and expanding the cell coverage area of B5G networks in [22–25]. Void BSs, which are not serving any users, coordinate to jointly transmit to cell edge users in a particular cell, thereby improving the SINR performances of all near and far NOMA users in [22]. In order to overcome ICI, [23] investigates a dynamic power allocation problem for sum-rate maximization in a multi-cell NOMA HetNet using CoMP. Analysis and study of the application of several CoMP NOMA models for power allocation in multi-cell settings have been conducted. According to [24,25], integrating JT-CoMP, NOMA, and heterogeneous cloud radio access networks (H-CRANs) improves SE. In [24], the idea of downlink dual connectivity utilizing millimetre wave and microwave links concurrently at front haul and access network in a CoMP NOMA H-CRAN to maximize EE is explored. In contrast to the static modeling of users and BSs based on simulation in [23], authors in [25] create a framework utilizing stochastic geometry. In particular, the deployment of user equipment (UE) and remote radio heads is modeled using Poisson point process to satisfy the topological and spatial randomness requirements of B5G cellular networks. A joint resource allocation problem and hybrid OMA/NOMA mode design is studied in [21]. Each user with two RX chains is served by two transmitting receiving points (TRPs) of a single BS using non-coherent joint transmission.

Authors in [22–27], consider QoS-based resource allocation for a NOMA-enabled JT-CoMP HetNet only. The research on combining NOMA and OMA in existing literature is fairly limited [21,28–32], the proposed methods are not adaptive approaches. In these works, either OMA/NOMA modes are fixed scenarios [21], or user clusters utilize NOMA and have orthogonal resources across cell clusters, or employ either OMA or NOMA for one channel realization [31], or pair all network users using NOMA and multiplex the remaining unpaired users using OMA [32]. In [33–35], the authors implement an adaptive hybrid OMA/NOMA scheme with user selection. This method is utilized in underlay cooperative networks, where the primary users set a threshold for acceptable interference. It effectively manages interference and achieves high throughput and spectrum efficiency for both near and far-users. However, it does not address interference for edge users in a multi-cell context. Authors in [36], consider SIC power consumption in the EE analysis but it is only for JT -CoMP NOMA. Moreover, they consider only one NOMA cluster under each BS. The evaluations are only for one CoMP user in the system.

Our work examines a multi-cell dynamic hybrid OMA/NOMA system. In our work, special attention is paid to users located specifically at the cell edges in order to mitigate interference by neighboring BSs, which further helps in extending the coverage area and signal strength of the weak bordering users. Each UE in the two-tier hybrid multiple-access (OMA/NOMA) enabled network experiences different types of interference. The management of cross-tier and co-tier interference coupled with inter NOMA user interference (INUI) especially at the

cell edges, is a challenging task. In our proposed hybrid multiple-access HetNet, we employ a non-coherent JT-CoMP at the secondary tier to avoid interference at the cell edges. At least two SBSs coarsely coordinate with each other to simultaneously transmit information to the weaker user. Based on the channel gains [37], the users in each small cell can be classified into two categories: (i) CoMP users and (ii) non-CoMP users. Further, depending upon the overall optimal rate policy, the BS can adaptively switch between OMA or NOMA. In case OMA is adopted, specific bandwidth is allocated to the SBS user equipment (SUE), whereas for NOMA, the power allocation coefficients are decided by the serving BS according to the channel gain difference of the paired users. Therefore, for each SUE, one of the following four modes is adopted to access the network in the hybrid approach: (a) non-CoMP NOMA user, (b) CoMP NOMA user, (c) non-CoMP OMA user, and (d) CoMP OMA user.

1.2. Motivation and contribution

While Coordinated Multi-Point (CoMP) Non-Orthogonal Multiple Access (NOMA) effectively addresses the spectral efficiency (SE), connectivity, and capacity requirements of users, particularly at the cell edges, CoMP Orthogonal Multiple Access (OMA) can mitigate inter-cell interference. Therefore, a hybrid Joint Transmission (JT)-CoMP enabled OMA/NOMA technique that combines the advantages of CoMP OMA and CoMP NOMA provides an adaptable and efficient solution moving forward. A detailed review of the existing literature reveals a significant gap in research on QoS-oriented resource allocation within non-coherent JT-CoMP-enabled hybrid multiple-access HetNet, particularly in terms of EE. This work aims to bridge this gap by providing the following contributions:

1. We investigate the integration of JT-CoMP and hybrid OMA/NOMA techniques for downlink transmission of HetNets, with a focus on improving service for edge users via SBSs coordination. Our work focuses on cell-edge interference in this novel multi-cell access model. In addition, we provide analytical expressions for users' data rates in the proposed hybrid OMA/NOMA network under various configurations, including non-CoMP NOMA, non-CoMP OMA, CoMP NOMA and CoMP OMA.
2. We develop an optimization framework to maximize EE while adhering to the constraints imposed by SIC, QoS, and available power budget. The optimization problem addresses the complex balance needed to optimize network performance under these constraints.
3. We propose a low complexity heuristic algorithm, referred to as Dynamic CoMP user selection with energy-efficient adaptive multiple access (DCEAMA) algorithm, to solve formulated mixed integer non-linear programming (MINLP) optimization problem. This algorithm strategically categorizes users in CoMP and non-CoMP, decides appropriate multi-access OMA or NOMA, selects the user pairing if required and allocates power to ensure the EE is maximized.
4. We evaluate the performance of EE using two different power allocation schemes: the uniform power allocation method (UPAM) which uses the total available power and divides it equally among all network users, and the optimized power consumption method (OPCOM), which aims to minimize the overall power consumption of the network. We evaluate the proposed approach for the power consumption of SIC in the context of near non-CoMP NOMA users to obtain more accurate and unbiased results.

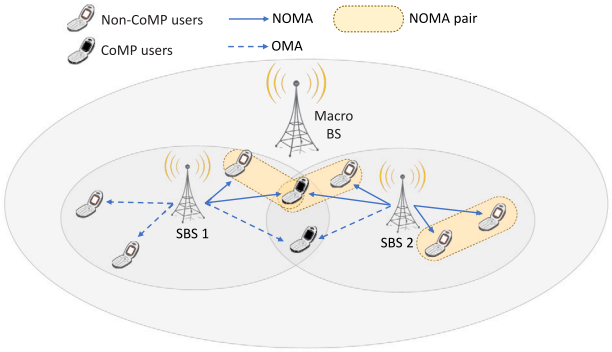

Fig. 1. Proposed system model.

Table 1
Table of notations.

Notations	Definition
$\mathcal{M}_s$	Set of SUEs under the coverage of sth SBS
S	Set of all SBSs
B	Bandwidth of a RB
N_o	Gaussian noise
α_{m_s}	NOMA/OMA binary indicator for user m_s
β_{m_s}	CoMP/non-CoMP binary indicator for user m_s
λ_{m_s}	Near/Far binary indicator for NOMA user m_s
$\lvert h_{m_s}^{(\bar{s})}\rvert^2$	Channel gain between SBS $\bar{s}$ and SUE m_s
$\theta_{m_s}^{\dagger}$	Power allocation coefficient of NOMA user for UPAM, where $\dagger \in \{N, F\}$
$p_{m_s}^{\dagger(\bar{s})}$	Transmit power from SBS $\bar{s}$ to m_s, where $\dagger \in \{N, F, O, OC, NC\}$
$\bar{P}$	Total power consumption of network
$\gamma_{m_s}^{\dagger}$	SINR of user m_s with SBS s, where $\dagger \in \{N, F, O, OC, NC\}$
$R_{m_s}^{\dagger}$	Achievable data rate of user m_s, where $\dagger \in \{N, F, O, OC, NC\}$
$\bar{R}$	Total achievable rate of network

1.3. Notations

Matrices are denoted by uppercase boldface letters or symbols, such as **H**. Variables are depicted using lowercase math-style letters, like h, and constants are indicated by uppercase math-style letters, such as B. Sets are denoted using calligraphic font, like $\mathcal{M}$. A lowercase subscript or superscript represents an index, for instance, in m_s, the subscript s denotes the index of the variable m. On the other hand, an uppercase subscript or superscript is employed to indicate an entire variable or notation; for example, "R^N" represents the entire notation. Table 1 provides the definitions for the notations used in this paper.

1.4. Paper organization

The paper is organized as follows. In Section 2, we present the proposed system model. In Section 3, the problem formulation for QoS based resource allocation is discussed. The power allocation schemes used in this work are discussed in Section 4. Section 5 provides a detailed explanation of the heuristic algorithm, referred to as DCEAMA algorithm, and its sub routines. The numerical analysis and discussion is addressed in Section 6. Finally, Section 7 concludes the paper and provides directions for future research.

2. System model

Consider a two tier JT-CoMP-enabled hybrid multiple-access OMA/NOMA HetNet, as shown in Fig. 1. A high-power macro base station

(MBS) is under-laid by a set of SBSs, represented as $\mathcal{S} = \{1, \ldots, S\}$. Each SBS, denoted by s, where $s \in \mathcal{S}$, provides coverage to randomly distributed SUEs. Every SUE served by SBS s is identified by an index m_s, where m represents the user index associated with that SBS s. Furthermore, the set of SUEs served by SBS s is denoted as $\mathcal{M}_s = \{1_s, 2_s, \ldots, M_s\}$, where M_s represents the total number of SUEs covered by SBS s. It is assumed that all BSs and SUEs employ a single antenna configuration. For downlink transmissions, each SBS selects users for scheduling through a hybrid multiple-access technique. Based on the varying conditions, it may utilize OMA or NOMA.

The resources at the backhaul of SBS have been pre-allocated using OMA. JT-CoMP is exclusively employed at the access link layer to accommodate edge users facing interference limitations. The channel between SBS $\bar{s} \in \mathcal{S}$ and SUEs m_s is characterized by Rayleigh fading which accounts for both distance and shadowing effects and is represented as $|h_{m_s}^{(\bar{s})}|^2$. The MBS assumes complete CSI knowledge, allowing it to make centralized decisions on user pairing, channel gains, CoMP strategies, power allocation, and selecting the optimal multiple-access approach. We assume that a maximum of two SBSs coordinate to support cell edge CoMP users [23,36], thereby mitigating interference and enhancing the QoS and EE for all network users. To simplify mathematical analysis and modeling in NOMA, perfect SIC is assumed. This approach focuses on user categorization, pairing, and power allocation. Each NOMA group includes two SUEs. To ensure efficient SIC and to optimize both the sum-rate and user fairness among all users within the coverage of SBS s, the SUEs are arranged in ascending order based on their channel gains, given as $|h_{1_s}^{(\bar{s})}|^2 < |h_{2_s}^{(\bar{s})}|^2 < \cdots < |h_{M_s}^{(\bar{s})}|^2$.

The goal of this work is to maximize EE by dynamically allocating power including JT-CoMP enabled hybrid multiple-access OMA/NOMA scenario. This scenario includes the JT and coordinated cooperation between two SBSs. Since the hybrid multiple-access approach is exclusively used within the secondary tier, this work considers two types of interference: INUI, and co-tier interference, referred to as ICI. Interference originating from a BS situated outside the coordinating set is regarded as part of the noise power. The total number of SUEs is categorized into CoMP and non-CoMP users, with each category further split into NOMA and OMA users. With randomly distributed SUEs, it is possible for a NOMA pair to be composed entirely of non-CoMP users, without including any CoMP SUE. Therefore, the non-CoMP SUEs can be paired with either CoMP users or non-CoMP users. This leads to two possible pairings: (a) {non-CoMP, CoMP} pairing, and (b) {non-CoMP, non-CoMP} pairing for SUEs. In such pairings, the non-CoMP SUEs can be categorized as either near-users or far-users, whereas the CoMP SUEs will always be classified as far-users. The NOMA pairs employ distinct orthogonal RBs, thereby eliminating any intra-cell interference. The bandwidth and power utilization of two non-CoMP users using NOMA and OMA is shown in Figs. 2(a) & 2(b) where as Figs. 2(c) and 2(d) display the bandwidth and power utilization of three CoMP, non-CoMP SUEs using NOMA and OMA both.

Based on network rate performance and channel conditions, four possible scenarios emerge where non-CoMP and CoMP SUEs may be grouped under NOMA or OMA modes to access the network. To ensure a fair comparison, we examine users in pairs, regardless of whether they adopt OMA or NOMA. Additionally, we assume that both SBSs serve the CoMP SUE using the same multiple-access technique, excluding the possibility of combining OMA from one SBS and NOMA from another. Below, we discuss these four cases and develop expressions for data rate.

2.1. NOMA clustering with non-CoMP users

If a NOMA pair comprises two non-CoMP users, they are identified as near-user and far-user, denoted as m_s and m'_s respectively, with both $\{m_s, m'_s\} \in \mathcal{M}_s$, based on their channel with the associated SBS s. The

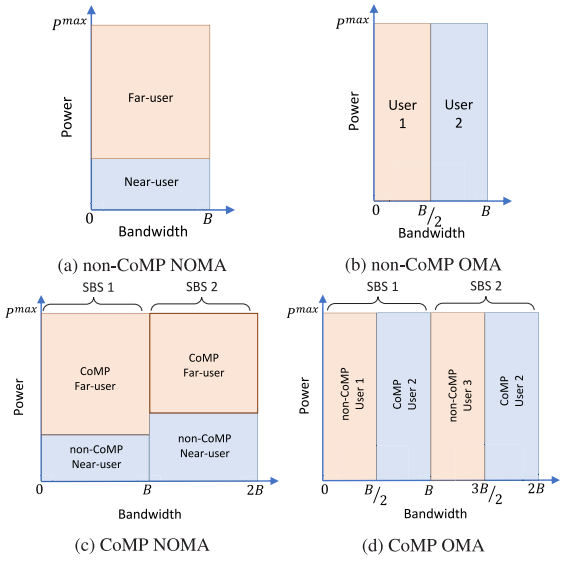

Fig. 2. Bandwidth and power allocation.

near-user employs SIC to effectively remove interference from the far-user's signal. The expressions for the SINR for the near-user, after a perfect SIC is give as,

$$\gamma_{m_s}^{N} = \frac{|h_{m_s}^{(s)}|^2 p_{m_s}^{N(s)}}{N_o}. \tag{1}$$

In the conventional NOMA, the far-user decodes the received signal directly, treating the signal from the near-user as interference. The SINR for the far-user is expressed as,

$$\gamma_{m'_s}^{F} = \frac{|h_{m'_s}^{(s)}|^2 p_{m'_s}^{F(s)}}{|h_{m'_s}^{(s)}|^2 p_{m_s}^{N(s)} + N_o}. \tag{2}$$

Finally, the achievable rates for SUEs m_s and m'_s, who are served over a shared unit RB, are calculated as follows:

$$R_{m_s}^{N} = B \log_2 \left(1 + \gamma_{m_s}^{N}\right), \tag{3}$$

and

$$R_{m'_s}^{F} = B \log_2 \left(1 + \gamma_{m'_s}^{F}\right), \tag{4}$$

We assume $B = 1$ Hz for each RB, indicating that the NOMA pair receives the entire bandwidth of RB.

2.2. OMA with non-CoMP users

Two non-CoMP OMA SUEs, denoted as m_s and m'_s, are served by a single SBS s over a dedicated RB. Consequently, there is no INUI and ICI between the SUEs in this scenario. Therefore, the signal to noise ratio (SNR) expression for user m_s is given as,

$$\gamma_{m_s}^{O} = \frac{|h_{m_s}^{(s)}|^2 p_{m_s}^{O(s)}}{N_o}, \tag{5}$$

and the data rate is expressed as,

$$R_{m_s}^{O} = B \log_2 \left(1 + \gamma_{m_s}^{O}\right). \tag{6}$$

The SNR and corresponding data rate expression for SUE m'_s are similar to (5) and (6), respectively. Considering NOMA configuration involving two SUEs, we include two OMA users for a fair and equitable comparison. For two non-CoMP OMA users, the bandwidth of the RB is equally divided between them, i.e., $B = 1/2$ Hz.

2.3. NOMA clustering with non-CoMP and CoMP users

A near non-CoMP user within the coverage range of SBS s, denoted as m_s, can be paired with a far CoMP user that receives service from two coordinating SBSs s and $\bar{s}$. The near non-CoMP NOMA user utilizes SIC to remove the interference caused by the far CoMP NOMA user. The SINR for the near non-CoMP user is calculated as in (1) after the perfect SIC has been applied.

To enhance network coverage and quality for cell-edge users, who experience lower signal strength, CoMP is utilized. The far CoMP NOMA user receives transmissions from two coordinating SBSs s and $\bar{s}$, and therefore, it can be represented as m'_s or $m'_{\bar{s}}$. The signal received by the far-user is represented as $|h^{(s)}_{m'_s}|^2 p^{NC(s)}_{m'_s} + |h^{(\bar{s})}_{m'_{\bar{s}}}|^2 p^{NC(\bar{s})}_{m'_{\bar{s}}}$. In this scenario, the CoMP user faces INUI from the near non-CoMP NOMA user. This interference is due to the CoMP user being involved in NOMA pairs with both SBSs, s and $\bar{s}$. The expression for SINR for the CoMP NOMA user is as follows:

$$\gamma^{NC}_{m'_s} = \frac{|h^{(s)}_{m'_s}|^2 p^{NC(s)}_{m'_s} + |h^{(\bar{s})}_{m'_{\bar{s}}}|^2 p^{NC(\bar{s})}_{m'_{\bar{s}}}}{|h^{(s)}_{m'_s}|^2 p^{N(s)}_{m_s} + |h^{(\bar{s})}_{m'_{\bar{s}}}|^2 p^{N(\bar{s})}_{m_{\bar{s}}} + N_o}. \tag{7}$$

The data rates for the near non-CoMP NOMA users m_s and $m_{\bar{s}}$ are calculated as in (3), whereas the data rate for far CoMP NOMA user is expressed,

$$R^{NC}_{m'_s} = B \log_2 \left(1 + \gamma^{NC}_{m'_s}\right). \tag{8}$$

2.4. OMA with CoMP users

As a CoMP-OMA user is served by coordinating SBSs s and SBS $\bar{s}$, it results in an enhanced received signal, represented as $|h^{(s)}_{m'_s}|^2 p^{OC(s)}_{m'_s} + |h^{(\bar{s})}_{m'_{\bar{s}}}|^2 p^{OC(\bar{s})}_{m'_{\bar{s}}}$. The SNR to the CoMP user is given as follows:

$$\gamma^{OC}_{m'_s} = \frac{|h^{(s)}_{m'_s}|^2 p^{OC(s)}_{m'_s} + |h^{(\bar{s})}_{m'_{\bar{s}}}|^2 p^{OC(\bar{s})}_{m'_{\bar{s}}}}{N_o}. \tag{9}$$

The data rate for the paired non-CoMP OMA SUE m_s is calculated as in (6). The achievable rate of the CoMP OMA user is given as,

$$R^{OC}_{m'_s} = B \log_2 \left(1 + \gamma^{OC}_{m'_s}\right), \tag{10}$$

where $B = 1/2$ Hz in this case.

2.5. Total rate and power consumption in the network

The total number of SUEs is classified into CoMP and non-CoMP users, with each category further divided into NOMA and OMA users. Furthermore, non-CoMP NOMA users are divided into near and far NOMA users. A unified rate expression that covers all four scenarios previously outlined is formulated by introducing the decision variables α_{m_s}, β_{m_s}, and λ_{m_s}. These binary indicators are defined as,

$$\begin{aligned}
\beta_{m_s} &= \begin{cases} 1, & \text{if user } m_s \text{ is a CoMP user} \\ 0, & \text{if user } m_s \text{ is a non-CoMP user} \end{cases} \\
\alpha_{m_s} &= \begin{cases} 1, & \text{if user } m_s \text{ is under OMA configuration} \\ 0, & \text{if user } m_s \text{ is under NOMA configuration} \end{cases} \\
\lambda_{m_s} &= \begin{cases} 1, & \text{if user } m_s \text{ is near NOMA user} \\ 0, & \text{if user } m_s \text{ is far NOMA user.} \end{cases}
\end{aligned} \tag{11}$$

Finally, the unified rate is expressed as,

$$\begin{aligned}
R_{m_s} = \beta_{m_s} \Big[\alpha_{m_s} R^{OC}_{m'_s} + \left(1 - \alpha_{m_s}\right) R^{NC}_{m'_s} \Big] + \\
\left(1 - \beta_{m_s}\right) \Big[\alpha_{m_s} R^{O}_{m_s} + \left(1 - \alpha_{m_s}\right) \left(\lambda_{m_s} R^{N}_{m_s} + \right. \\
\left. \left(1 - \lambda_{m_s}\right) R^{F}_{m_s} \right) \Big].
\end{aligned} \tag{12}$$

The same rate expression will be used to calculate the data rate of both paired users, denoted as m_s and m'_s. The potential outcomes of the decision variables α_{m_s}, β_{m_s} and λ_{m_s} are summarized in Table 2. For instance, $\alpha_{m_s} = 0$, $\beta_{m_s} = 0$ and $\lambda_{m_s} = 1$ indicates that the user m_s is selected as a near non-CoMP NOMA user. This user can be paired with a distant user m'_s that can either be non-CoMP or CoMP NOMA user. In both cases, $\alpha_{m_s} = 0$ indicates that the same multiple-access scheme is applied to the near-user and the other user in the pairing. When β_{m_s} equals to 1, λ_{m_s} must be zero, indicating that a CoMP user must be a far-user.

Assuming there are W_s pairs of users under each SBS. Then, the total achievable data rate of a hybrid multiple-access network enabled with JT-CoMP is given as,

$$\bar{R} = \sum_{s \in S} \sum_{\{m_s, m'_s\} \in \mathcal{W}_s} \left\{ R_{m_s} + R_{m'_s} \right\}, \tag{13}$$

where $\{m_s, m'_s\}$ denotes an arbitrary pair of users in set $\mathcal{W}_s$. The network's total power consumption is separated into two parts: the adaptable transmit power of SBS, represented as $p^{\dagger(s)}_{m_s}$, and the constant power consumption of the network's circuitry, denoted as P^{circ}. Because SIC is implemented only at the strong users, the P^{circ} may differ for each SUE. However, for the sake of simplicity, it is assumed to be constant for all possible SUE scenarios. The total transmit power P_T of all SBSs is given as,

$$P_T = \sum_{s \in S} \sum_{m_s \in \mathcal{M}_s} \left(p^{N(s)}_{m_s} + p^{F(s)}_{m'_s} + p^{NC(\bar{s})}_{m'_s} + p^{O(s)}_{m_s} + p^{OC(\bar{s})}_{m'_s} \right), \tag{14}$$

and the overall power consumption of the network is expressed as:

$$\bar{P} = P_T + P^{circ}. \tag{15}$$

2.6. Energy efficiency of the network

One of the key performance indicators of a cellular network is its EE. The network's EE can be expressed as the ratio of the total sum data rate to the total consumed power. Mathematically, it can be expressed as,

$$\begin{aligned}
\varepsilon &= \frac{\text{Total achievable rate}}{\text{Total consumed power}} = \frac{\bar{R}}{\bar{P}} \\
&= \frac{\sum_{s \in S} \sum_{\{m_s, m'_s\} \in \mathcal{W}_s} \left\{ R_{m_s} + R_{m'_s} \right\}}{P_T + P^{circ}}.
\end{aligned} \tag{16}$$

3. Problem formulation

This section presents a joint dynamic power allocation optimization problem to maximize EE in a JT-CoMP enabled hybrid multiple-access HetNet. We consider QoS, SIC, and power consumption constraints to achieve the goal. Consequently, the optimization problem can be formulated as:

$$\begin{aligned}
\mathbf{OP}: \ & \max_{\boldsymbol{\alpha}, \boldsymbol{\beta}, \boldsymbol{\lambda}, \mathbf{P}} \ \boldsymbol{\varepsilon} \\
& \text{subject to:} \\
& \mathbf{C_1}: 0 \le p^{\dagger(s)}_{m_s} \le P^{max}, \ \forall s, m_s, \\
& \mathbf{C_2}: \sum_{m_s \in \mathcal{M}_s} p^{\dagger(s)}_{m_s} \le P^{max}, \ \forall s, \\
& \mathbf{C_3}: R_{m_s} \ge R^{min}, \ \forall s, m_s, \\
& \mathbf{C_4}: \lambda_{m_s} \le |1 - \beta_{m_s} - \alpha_{m_s}|, \ \forall s, m_s, \\
& \mathbf{C_5}: p^{\dagger(s)}_{m'_s} |h^{(s)}_{m_s}|^2 - p^{\dagger(s)}_{m_s} |h^{(s)}_{m_s}|^2 \ge P^{SIC}, \ \forall s, m_s, \\
& \mathbf{C_6}: \alpha_{m_s}, \ \beta_{m_s}, \ \lambda_{m_s} \in \{0, 1\}, \ \forall s, m_s,
\end{aligned} \tag{17}$$

Table 2
Users' categorization w.r.t. α_{m_s}, β_{m_s} and λ_{m_s}.

	OMA, $\alpha_{m_s}=1$	**NOMA**, $\alpha_{m_s}=0$	
CoMP, $\beta_{m_s}=1$	$R^{OC}_{m'_s}$	$R^{NC}_{m'_s}$	
non-CoMP, $\beta_{m_s}=0$	$R^{O}_{m_s}$	**Near-user**, $\lambda_{m_s}=1$	**Far-user**, $\lambda_{m_s}=0$
		$R^{N}_{m_s}$	$R^{F}_{m'_s}$

where the matrix $\mathbf{P}^{(s)}$ represents the optimal transmit power from SBS s to the users and can be expressed as:

$$\mathbf{P}^{(s)}=\begin{bmatrix} p^{\dagger(s)}_{1_s} & p^{\dagger(s)}_{2_s} & \cdots & p^{\dagger(s)}_{M_s} \\ p^{\dagger(s)}_{1_{\bar{s}}} & p^{\dagger(s)}_{2_{\bar{s}}} & \cdots & p^{\dagger(s)}_{M_{\bar{s}}} \end{bmatrix}, \tag{18}$$

where $\dagger \in \{N, F, O, OC, NC\}$. The notations $\{N, F, O, OC, NC\}$ correspond to near NOMA, far NOMA, OMA, OMA CoMP and NOMA CoMP respectively. In (17), R^{min} denotes the minimum rate requirement of the SUEs, and P^{max} represents the maximum power budget available at each SBS. Constraint $\mathbf{C_1}$ ensures that the power allocated to each user m_s is within the range $[0, P^{max}]$, indicating that it should be non-negative and not exceed the maximum available power. Constraint $\mathbf{C_2}$ limits the total assigned power to all users from exceeding the maximum available power. Constraint $\mathbf{C_3}$ guarantees the QoS for every user. It states that the minimum data rate requirement R^{min} must be achieved by each user. The constraint $\mathbf{C_4}$ states that if a CoMP user uses NOMA configuration, it must be a far-user. Given the ordering of SUEs is based on their channel gain, the SIC constraint in $\mathbf{C_5}$ applies to near non-CoMP SUEs. The transmit power for a weaker user needs to be higher than the combined power of all users with stronger channel gains within a cluster. Necessary power constraints for efficient SIC for a two user NOMA pair to cancel the interference from $p^{\dagger(s)}_{m'_s}$ to the $p^{\dagger(s)}_{m_s}$ receiver is enforced by $\mathbf{C_5}$, where P^{SIC} represents the minimal threshold power difference necessary to distinguish between the decodable signal and non-decodable NOMA interference. Constraint $\mathbf{C_6}$ shows the lower and upper bounds of the decision variables.

Finally, the objective function is to maximize the network's EE while satisfying the practical constraints $\mathbf{C_1}$ through $\mathbf{C_6}$. The optimization problem **OP** in (17) is MINLP in nature. Solving MINLP problems involves complexities arising from the coexistence of nonlinear functions and decision variables of a mixed nature. To tackle these complexities, we adopt a systematic approach to resolve the optimization process, including user classification, CoMP/non-CoMP pairing, multiple-access method selection, and power allocation.

4. Power allocation schemes

We evaluate the network's EE performance with two power consumption schemes. The baseline model, called UPAM, distributes power evenly among all users and serves as a benchmark for comparisons. The OPCOM power allocation scheme optimizes EE by minimizing power usage to meet users' rate demands. This technique eventually improves resource utilization to optimize network performance. We evaluate both power allocation schemes across CoMP OMA, CoMP NOMA, and the hybrid JT-CoMP OMA/NOMA models to ensure a fair comparison. The two power allocation schemes for EE calculation are as follows:

4.1. Uniform power allocation method (UPAM)

In this scheme, the total power budget at each SBS is uniformly distributed across all users associated with it. Power must be distributed among each pair of users using both OMA and NOMA techniques. This step is critical to establishing the foundation for future strategic decisions. Given that each pair consists of two users, the power allocated to each pair is $2.p^{\dagger(s)}_{m_s}$. In OMA, power is assigned evenly among both users in the pair. However, in NOMA, power is shared among the near and far-users with the ratio of $\theta^{N}_{m_s}$ and $\theta^{F}_{m'_s}$, respectively. The power coefficients $\theta^{N}_{m_s}$ and $\theta^{F}_{m'_s}$ are determined so that the target rate R^{min} must be achieved, i.e., $R^{N}_{m_s} \geq R^{min}$. The target rate for the far NOMA user is defined as,

$$R^{min}=\log_2\left(1+\frac{|h^{(s)}_{m'_s}|^2\cdot\theta^{F}_{m'_s}\cdot p^{\dagger(s)}_{m_s}}{|h^{(s)}_{m'_s}|^2\cdot\theta^{N}_{m_s}\cdot p^{\dagger(s)}_{m_s}+N_o}\right), \tag{19}$$

which can be written as,

$$2^{R^{min}}=1+\frac{|h^{(s)}_{m'_s}|^2\cdot\theta^{F}_{m'_s}\cdot p^{\dagger(s)}_{m_s}}{|h^{(s)}_{m'_s}|^2\cdot\theta^{N}_{m_s}\cdot p^{\dagger(s)}_{m_s}+N_o},$$

$$2^{R^{min}}-1=\frac{|h^{(s)}_{m'_s}|^2\cdot\theta^{F}_{m'_s}\cdot p^{\dagger(s)}_{m_s}}{|h^{(s)}_{m'_s}|^2\cdot\theta^{N}_{m_s}\cdot p^{\dagger(s)}_{m_s}+N_o},$$

$$\mu=\frac{|h^{(s)}_{m'_s}|^2\cdot\theta^{F}_{m'_s}\cdot p^{\dagger(s)}_{m_s}}{|h^{(s)}_{m'_s}|^2\cdot\theta^{N}_{m_s}\cdot p^{\dagger(s)}_{m_s}+N_o}, \tag{20}$$

where $\mu=2^{R^{min}}-1$. After algebraic simplification, the power coefficient for the far-user can be expressed as,

$$\theta^{F}_{m'_s}=\frac{\mu\left(|h^{(s)}_{m_s}|^2\cdot p^{\dagger(s)}_{m_s}+N_o\right)}{|h^{(s)}_{m_s}|^2\cdot p^{\dagger(s)}_{m_s}(1+\mu)}. \tag{21}$$

Furthermore, $\theta^{N}_{m_s}+\theta^{F}_{m'_s}=1$ and $\theta^{N}_{m_s}\ll\theta^{F}_{m'_s}$ to increase the probability of perfect decoding of desired signals at both users. Therefore, $\theta^{N}_{m_s}$ can be computed as:

$$\theta^{N}_{m_s}=1-\theta^{F}_{m'_s}. \tag{22}$$

4.2. Optimized power consumption method (OPCOM)

This power allocation scheme evaluates network's EE performance by allocating optimal power to each user based on their rates. The computed power should be sufficient to satisfy a user's QoS criteria. For non-CoMP near and far NOMA users, the optimal power can be calculated as,

$$p^{N(s)}_{m_s}=\frac{\mu N_o}{|h^{(s)}_{m_s}|^2}, \tag{23}$$

and

$$p^{F(s)}_{m'_s}=\frac{\mu\left(|h^{(s)}_{m'_s}|^2 p^{N(s)}_{m_s}+N_o\right)}{|h^{(s)}_{m'_s}|^2}. \tag{24}$$

To calculate the optimal power allocation CoMP NOMA expressions for both coordinating SBSs, we consider $p^{NC(s)}_{m'_s}=p^{NC(\bar{s})}_{m'_{\bar{s}}}$ and derive it as

$$p^{NC(s)}_{m'_s}=\frac{\mu\left(|h^{(s)}_{m'_s}|^2 p^{N(s)}_{m_s}+|h^{(\bar{s})}_{m'_{\bar{s}}}|^2 p^{N(s)}_{m_{\bar{s}}}+N_o\right)}{|h^{(s)}_{m'_s}|^2+|h^{(\bar{s})}_{m'_{\bar{s}}}|^2}. \tag{25}$$

For users using OMA, we need to modify the constant minimum rate requirement value from μ to τ because we assume $B=1/2$, such that

$$\tau=2^{(2\cdot R^{min})}-1. \tag{26}$$

The non-CoMP OMA expression for power is given as,

$$p^{O(s)}_{m_s}=\frac{\tau N_o}{|h^{(s)}_{m_s}|^2}, \tag{27}$$

Algorithm 1: DCEAMA Algorithm

1 **Initialization:** P^{max}, R^{min}
2 Set of SUEs, $\mathcal{M}_s = \{1_s, \ldots, M_s\}$, $s \in \{1,2\}$, such that $\mathcal{M}_1 \cup \mathcal{M}_2 = \mathcal{M}$
3 Estimated channel gains, $\mathbf{H}^{(\bar{s})} = |h_{m_s}^{(\bar{s})}|^2$, $\forall s, \bar{s} \in \mathcal{S}$
4 $\{\mathcal{X}, c, \boldsymbol{\beta}\} \leftarrow$ **Call** CoMP_Count($\mathcal{M}, \mathbf{H}$)
5 $\{\mathcal{A}, \mathcal{B}\} \leftarrow$ **Call** CnC_Pairing($\mathcal{M}, \mathcal{X}, \mathbf{H}, c$)
6 Classify users within each pair in $\mathcal{B}$ as near-user ($\lambda_{m_s} = 1$) and far-user ($\lambda_{m_s} = 0$) according to $\mathbf{H}$
7 $\boldsymbol{\alpha} \leftarrow$ **Call** MASON($\mathcal{M}, \mathcal{A}, \mathcal{B}, \lambda, \boldsymbol{\beta}, \mathbf{H}$)
8 Compute the overall system EE using (16) with UPAM
9 Compute optimal powers for non-CoMP near and far NOMA SUEs using (23), (24), and CoMP NOMA SUEs using (25) within feasible region
10 Compute optimal powers for non-CoMP OMA SUEs using (27), and CoMP OMA SUEs using (28) within feasible region
11 Compute overall system EE using (16) OPCOM

Algorithm 2: CoMP_Count

Input: $\mathcal{M}$, $\mathbf{H}$
Output: $\mathcal{X}$, c, $\boldsymbol{\beta}$
1 **Initialization:** $\mathcal{X} = \emptyset$: Set of CoMP users, c: Total no. of CoMP users, Φ : CoMP detection threshold, $\boldsymbol{\beta} = 0$: CoMP/non-CoMP user indicator
2 **Define:** $|h_{m_s}^{(\bar{s})}|^2 \in \mathbf{H}$, $\forall s, \bar{s} \in \mathcal{S}$, $\beta_{m_s} \in \boldsymbol{\beta}$, $\forall m_s, s$
3 $c = 0$
4 **foreach** $s \in \{1,2\}$ **do**
5 **foreach** $m_s \in \mathcal{M}_s$ **do**
6 **if** $||h_{m_s}^{(1)}|^2 - |h_{m_s}^{(2)}|^2| \leq \Phi$ **then**
7 $\mathcal{X}_s = \mathcal{X}_s \cup m_s$
8 $\beta_{m_s} = 1$
9 $c = c + 1$
10 $\mathcal{X} \leftarrow \mathcal{X} \cup \mathcal{X}_s$, $\boldsymbol{\beta} \leftarrow \boldsymbol{\beta} \cup \beta_{m_s}$

where it is the same for both paired users. To derive CoMP OMA minimal power consumption expression, we consider $p_{m'_s}^{OC(s)} = p_{m'_{\bar{s}}}^{OC(\bar{s})}$, and is expressed as

$$p_{m'_s}^{OC(s)} = \frac{\tau N_o}{|h_{m'_s}^{(s)}|^2 + |h_{m'_{\bar{s}}}^{(\bar{s})}|^2}. \tag{28}$$

5. Proposed DCEAMA algorithm

In this section, we discuss the proposed heuristic algorithm, referred to as DCEAMA algorithm, as shown in Algorithm 1. The algorithm solves the complex optimization problem in steps, including user classification, user pairing, multiple-access selection, and power optimization. The sets of the randomly deployed SUEs within the coverage range of two SBSs are denoted as $\mathcal{M}_1$ and $\mathcal{M}_2$, where $\mathcal{M}_1 \cup \mathcal{M}_2 = \mathcal{M}$, and $\mathcal{M}$ represents the set of all users in the network. Channel gains between the users and the SBSs are estimated, such that the channel gains between SBSs s with users m_s and $m_{\bar{s}}$ are given as $|h_{m_s}^{(s)}|^2$ and $|h_{m_{\bar{s}}}^{(s)}|^2$, respectively. Similarly, the estimated channel gains of all users with the SBS s are represented by a matrix $\mathbf{H}^{(s)}$, which is defined as

$$\mathbf{H}^{(s)} = \begin{bmatrix} |h_{1_s}^{(s)}|^2 & |h_{2_s}^{(s)}|^2 & \ldots & |h_{M_s}^{(s)}|^2 \\ |h_{1_{\bar{s}}}^{(s)}|^2 & |h_{2_{\bar{s}}}^{(s)}|^2 & \ldots & |h_{M_{\bar{s}}}^{(s)}|^2 \end{bmatrix}. \tag{29}$$

Algorithm 3: CnC_Pairing

Input: $\mathcal{M}$, $\mathcal{X}$, $\mathbf{H}$, c
Output: $\mathcal{A}$, $\mathcal{B}$
1 **Define:** $\mathcal{X}_s \in \mathcal{X}$, $\mathcal{M}_s \in \mathcal{M}$, $\forall s \in \mathcal{S}$
/* Pairing of CoMP and non-CoMP users */
2 $\mathcal{X} = \mathcal{X}_1 \cup \mathcal{X}_2$, after sorting $\mathcal{X}_1$, $\mathcal{X}_2$ individually
3 **foreach** $s \in \{1,2\}$ **do**
4 $\mathcal{Y}_s = \mathcal{M}_s - \mathcal{X}_s$ ▷ non-CoMP users
5 **if** $\mathcal{X}$ *is not empty* **then**
6 $\bar{\mathcal{A}}$ = Sort $\mathcal{Y}_s$ in ascending order according to $\mathbf{H}^{(s)}$
7 $\mathcal{A}_s \leftarrow$ Pair first c users in $\bar{\mathcal{A}}$ with CoMP users in $\mathcal{X}$
8 $\mathcal{Y}_s = \bar{\mathcal{A}}-$ {non-CoMP paired users in s}
/* Pairing of non-CoMP users */
9 **foreach** $s \in \{1,2\}$ **do**
10 **while** $\mathcal{Y}_s$ *not emptied* **do**
11 $\mathcal{B}_s \leftarrow$ Pair first and last users in $\mathcal{Y}_s$
12 $\mathcal{Y}_s \leftarrow \mathcal{Y}_s - \mathcal{B}_s$

The proposed DCEAMA algorithm detects CoMP SUEs in each SBS using $\mathbf{H}^{(s)}$ (line 4). To conduct a fair comparison for dynamically switching between OMA and NOMA, we build user pairings for both schemes, while in general only NOMA requires this pairing. Therefore, we construct pairings for non-CoMP and CoMP users, which are identified by Algorithm 2 (line 4). Algorithm 3 forms users' pairs and divides the pairs into two sets $\mathcal{A}$ and $\mathcal{B}$. (line 5). Set $\mathcal{A}$ includes both CoMP and non-CoMP users' pairs, but $\mathcal{B}$ only contains non-CoMP users' pairs. Following this, the set of users in $\mathcal{B}$ are classified as near and far-users according to their channel gains (line 6). Within each pair of users in $\mathcal{B}$, users with high channel gain are assigned $\lambda_{m_s} = 1$ and are categorized as near-users, whereas users with low gain are assigned $\lambda_{m_s} = 0$ and categorized as far-users. Then, the optimized multiple-access scheme (OMA or NOMA) is determined for each pair in $\mathcal{A}$ and $\mathcal{B}$ using Algo 4 (line 7). The network's EE is calculated with UPAM (line 8). After categorizing users as NOMA or OMA, the optimized power allocation, known as OPCOM, is calculated for each user (line 9 – 10). The optimized power for users in each pair in $\mathcal{A}$ and $\mathcal{B}$ is computed for NOMA pairings using (23), (24) and (25), and for OMA pairs using (27) and (28). Finally, the network's EE is determined using optimal resource allocation for all pairings, as given in (16).

The following subsections explain the subroutines used in Algorithm 1.

5.1. CoMP _Count algorithm: User identification and categorization

Algorithm 2 generates a set of CoMP users $\mathcal{X}$ and counts the total number of CoMP users in the network in c. Furthermore, the algorithm generates a binary indicator variable, $\boldsymbol{\beta}$, to categorize users as CoMP or non-CoMP users. It receives the set of all users, denoted as $\mathcal{M}$, and the channel matrix, represented as $\mathbf{H} = \{\mathbf{H}^{(1)}, \mathbf{H}^{(2)}\}$ as inputs. For SBS s, the algorithm classifies CoMP users by comparing the gain difference between users and their associated SBS s, as well as a coordinating SBS $\bar{s}$, against the given CoMP detection threshold, Φ (lines 4 – 10). Users with a gain difference less than Φ are identified as CoMP users (line 7) and their corresponding β_{m_s} is set to 1 (line 8). Additionally, the number of CoMP users for the respective SBS is also incremented (line 9). The same process is repeated for the other SBS.

5.2. CnC_Pairing algorithm: CoMP and non-CoMP pairing

The users are paired in Algorithm 3, using the 2-user downlink pairing, as proposed in [38]. This algorithm accepts the following

inputs: the set of all users $\mathcal{M}$, set of all CoMP users $\mathcal{X}$, channel matrix $\mathbf{H} = \{\mathbf{H}^{(1)}, \mathbf{H}^{(2)}\}$, and the total number of CoMP users c. It is assumed that the total number of CoMP users is always less than the number of non-CoMP users under each SBS. It produces two sets of pairings: $\mathcal{A}$ and $\mathcal{B}$. Set $\mathcal{A}$ contains the pairs of non-CoMP and CoMP users, whereas set $\mathcal{B}$ has exclusively non-CoMP user pairings. The following points are assumed for pairing.

- A pair must include exactly two users.
- Non-CoMP users cannot appear in multiple pairs.
- Non-CoMP users in a pair must be associated with the same SBS.
- The CoMP user is served by two SBSs, therefore it is paired with two different non-CoMP users associated with different SBSs.
- A CoMP user can only pair with a non-CoMP user.
- The unpaired users will select OMA as the multiple-access technology.

The algorithm begins with pairing of CoMP and non-CoMP users (lines 2 – 8). The CoMP users within each SBS, denoted as $\mathcal{X}_1$ and $\mathcal{X}_2$, are organized in ascending order based on their channel gains. Subsequently, these sets are merged to form $\mathcal{X}$ (line 2). For SBS s, the non-CoMP users $\mathcal{Y}_s$ are found by subtracting the set of CoMP users $\mathcal{X}_s$ from the total number of users associated $\mathcal{M}_s$ with s (line 4). If there exists any CoMP users in the network, i.e. $\mathcal{X} \neq \emptyset$, the pairing procedure will proceed, and the CoMP users are paired with non-CoMP users (lines 6 – 8). The users in $\mathcal{Y}_s$ are sorted in an increasing order according to channel gains (line 6). Then each CoMP user in $\mathcal{X}$ is paired with non-CoMP users of SBS s in $\mathcal{Y}_s$, and these pairs are then assigned to $\mathcal{A}_s$ (line 7). To prevent duplicates, paired users are removed from $\mathcal{Y}_s$ before identifying the next pairs, and $\mathcal{Y}_s$ is updated (line 8).

After the pairing of CoMP users with non-CoMP users is finished, the pairing of unpaired non-CoMP users within $\mathcal{Y}_s$ begins (lines 9 – 12). Because the users in $\mathcal{Y}_s$ are ordered based on channel gains, the first and last users for each SBS are paired and placed in $\mathcal{B}_s$ (line 11). The paired users are then removed from $\mathcal{Y}_s$ to prevent duplicates. The process continues until all users are paired, and $\mathcal{Y}_s$ is empty.

5.3. MASON algorithm: NOMA and OMA modes selection

The MASON Algorithm, shown in Algorithm 4, uses a hybrid multiple-access strategy, categorizing network users as OMA or NOMA configurations. The algorithm chooses the configuration that results in the highest sum rate per pair, which is affected by channel conditions and the number of users within a given cell. The algorithm takes in various inputs, including a set of users $\mathcal{M}$, pairs of {CoMP, non- CoMP} $\mathcal{A}$ and {non-CoMP, non-CoMP} $\mathcal{B}$, near/far binary indicator matrix λ, binary indicator matrix for CoMP/non-CoMP categorization $\boldsymbol{\beta}$, and a channel matrix $\mathbf{H} = \{\mathbf{H}^{(1)}, \mathbf{H}^{(2)}\}$. The algorithm outputs the optimal multiple-access technique for each pair, denoted as $\boldsymbol{\alpha}$. The power budget is equally distributed across all users associated with each SBS (line 3). Given that each pair consists of two users, the power allocated to each pair in both $\mathcal{A}$ and $\mathcal{B}$ is $2.p_{m_s}^{\dagger(s)}$ (line 4). Power allocation for each user pair is performed independently under both potential multiple-access techniques (OMA and NOMA), establishing the foundation for subsequent decisions. These decisions rely primarily on UPAM. The algorithm starts with deciding for multiple-access configuration for {CoMP, non-CoMP} pairings within $\mathcal{B}$ for both SBSs separately (lines 5–13). Therefore, for an arbitrary pair $\{m_s, m'_s\} \in \mathcal{B}_s$, the optimal power coefficients for the near-users $\theta_{m_s}^N$ and for the far-user $\theta_{m'_s}^F$ is calculated as in (21).

The sum data rate of a non-CoMP NOMA pair is derived using (3) and (4), and is given as,

$$R_{SUM}^{(1)} = R_{m_s}^N + R_{m'_s}^F. \tag{30}$$

Algorithm 4: MASON

Input: $\mathcal{M}$, $\mathcal{A}$, $\mathcal{B}$, λ, $\boldsymbol{\beta}$, $\mathbf{H}$
Output: $\boldsymbol{\alpha}$
1 **Define:** $\alpha_{m_s} \in \boldsymbol{\alpha}$, $\forall m_s, s$
2 $\boldsymbol{\alpha} = \emptyset$
3 $p_{m_s}^{\dagger(s)} = \frac{P^{max}}{|\mathcal{M}_s|}$, $\forall m_s \in \mathcal{M}_s$, $s \in \mathcal{S}$
4 Allocate $(2 \cdot p_{m_s}^{\dagger(s)})$ to each SUE pair in $\mathcal{A}_s, \mathcal{B}_s$, $\forall m_s, s$
/* NOMA/OMA decision for non-CoMP pairs */
5 **foreach** $s \in \{1, 2\}$ **do**
6 **foreach** *pair* $\{m_s, m'_s\} \in \mathcal{B}_s$ **do**
7 Calculate $(\theta_{m_s}^N, \theta_{m'_s}^F)$ for m_s, m'_s using (21)
8 $R_{SUM}^{(1)} \leftarrow$ Compute rates of m_s, m'_s using (30)
9 $R_{SUM}^{(2)} \leftarrow$ Compute rates of m_s, m'_s using (31)
10 **if** $R_{SUM}^{(1)} \geq R_{SUM}^{(2)}$ **then**
11 $\{\alpha_{m_s}, \alpha_{m'_s}\} = \{0, 0\}$
12 **else**
13 $\{\alpha_{m_s}, \alpha_{m'_s}\} = \{1, 1\}$
/* NOMA/OMA decision for mixed pairs */
14 **foreach** *pair* $\{m_1, m'_1\} \in \mathcal{A}_1$ *and* $\{m_2, m'_2\} \in \mathcal{A}_2$ **do**
15 Calculate $(\theta_{m_s}^N, \theta_{m'_s}^F)$ for m_s, m'_s using (21)
16 $R_{SUM}^{(3)} \leftarrow$ Compute rates of $\{m_1, m'_1\}$, $\{m_2, m'_2\}$ using (32)
17 $R_{SUM}^{(4)} \leftarrow$ Compute rates of $\{m_1, m'_1\}$, $\{m_2, m'_2\}$ using (33)
18 **if** $R_{SUM}^{(3)} \geq R_{SUM}^{(4)}$ **then**
19 $\{\alpha_{m_1}, \alpha_{m'_1}\} = \{0, 0\}$, $\{\alpha_{m_2}, \alpha_{m'_2}\} = \{0, 0\}$
20 **else**
21 $\{\alpha_{m_1}, \alpha_{m'_1}\} = \{1, 1\}$, $\{\alpha_{m_2}, \alpha_{m'_2}\} = \{1, 1\}$

Similarly, the sum data rate for two non-CoMP OMA paired users is calculated using (6), and is given as,

$$R_{SUM}^{(2)} = R_{m_s}^O + R_{m'_s}^O. \tag{31}$$

If $R_{SUM}^{(1)} > R_{SUM}^{(2)}$, the pair $\{m_s, m'_s\}$ is configured under NOMA mode (line 11); otherwise, the pair is configured under OMA mode (line 13). The same procedure is repeated for all pairs in $\mathcal{B}_s$.

Furthermore, the algorithm determines the mode decision for CoMP and non-CoMP paired users (line 14 – 21). In this scenario, pairings can only use NOMA or OMA configurations. Using (3) and (8), the sum data rate for NOMA clustering with two non-CoMP and a single (common) CoMP user can be computed as follows:

$$R_{SUM}^{(3)} = R_{m_s}^N + R_{m_{\bar{s}}}^N + R_{m'_s}^{NC}. \tag{32}$$

Similarly, using (6) and (10), the sum data rate for OMA pairs with a (common) CoMP user and two non-CoMP users can be computed as follows:

$$R_{SUM}^{(4)} = R_{m_s}^O + R_{m_{\bar{s}}}^O + R_{m'_s}^{OC}. \tag{33}$$

If $R_{SUM}^{(3)} > R_{SUM}^{(4)}$, the three users are configured under NOMA mode (line 19); otherwise, the users are configured under OMA mode. The same procedure is repeated for all pairs in $\mathcal{A}_1$ and $\mathcal{A}_2$.

5.4. Complexity of the algorithm

Algorithm 2 serves as a user classifier with a complexity of $O(S \cdot M_s)$. Since the user classification is performed over all SUEs, $m_s \in \mathcal{M}_s$, for all SBSs.

Algorithm 3 performs pairing of CoMP, non-CoMP users for each SBS. The sets $\mathcal{X}_1$ and $\mathcal{X}_2$ are sorted individually using the Merge sort

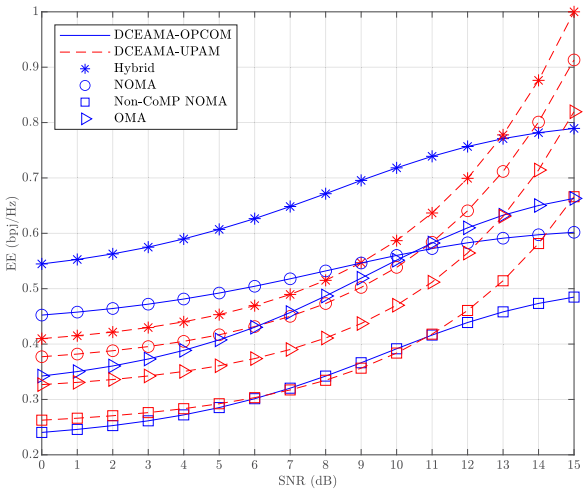

Fig. 3. EE without considering SIC power.

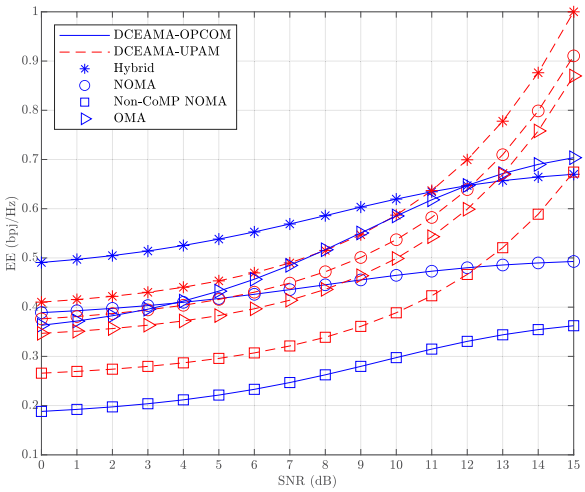

Fig. 4. EE considering SIC power.

algorithm. Therefore, the complexity is given as $O(|\mathcal{X}_1|\log|\mathcal{X}_1|)$ and $O(|\mathcal{X}_2|\log|\mathcal{X}_2|)$ for sorting individual sets, and the total complexity will be $O\left(|\mathcal{X}_1|\log|\mathcal{X}_1|+|\mathcal{X}_2|\log|\mathcal{X}_2|\right)$. In the loop between lines 3–8, the subtraction of sets on line 4 has a complexity of $O\left(M_s+|\mathcal{X}_s|\right)$. The sorting of $\mathcal{Y}_s$ on line 6 with complexity $|\mathcal{Y}_s|\log|\mathcal{Y}_s|$. Therefore, the overall complexity of the loop is given as $O\left(M_s+|\mathcal{X}_s|+|\mathcal{Y}_s|\log|\mathcal{Y}_s|\right)$. The worst-case complexity of the nested loops between lines 9 and 12 can be given as $O\left(2\cdot|\mathcal{Y}_s|/2\right)=O\left(|\mathcal{Y}|_s\right)$. Therefore, the overall complexity of Algorithm 3 is given as $O\left(M_s+|\mathcal{X}_s|+|\mathcal{Y}_s|\log|\mathcal{Y}_s|+|\mathcal{Y}|_s\right)$.

In Algorithm 4, the complexity is mainly dependent on $|\mathcal{A}_s|$, which represents the number of CoMP, non-CoMP users pairs, and $|\mathcal{B}_s|$, which represents the non-CoMP, non-CoMP user pairs in both SBSs. $\mathcal{A}_s$ and $\mathcal{B}_s$ are both bounded by the total number of users $|M_s|$. Assuming that all operations within the loops represent constant operations, the worst-case complexity for this algorithm is also $O(S\cdot M_s+M_s)$. Finally, after combining the complexity of individual routines, the overall complexity can be given as $O(S\cdot M_s+M_s\log M_s)$.

6. Simulation results and discussions

This section evaluates the performance of the proposed solution, known as DCEAMA, using UPAM and OPCOM power allocation schemes. UPAM scheme is used as a benchmark to evaluate system performance. Given the randomness in the system, Monte Carlo simulations are used to average the results. The benchmark resource allocation schemes employing only CoMP OMA, only CoMP NOMA and fully non-CoMP NOMA are also included. We consider a multi-cell system where a single MBS is under laid by 2 partly overlapping SBSs [23], each with 5 associated users. Each RB multiplexes at the most 2 users per pair. Rayleigh fading is used to model the channel at a small scale. Each SBS is assumed to have a transmit power of 25 dBm [23], and they all serve the same number of users. We assume SIC power and the circuitry power P^{circ} to be 10 dBm and 20 dBm [39], respectively. The minimum rate requirement, i.e., R^{min}, for each SUE normalized by bandwidth is defined as 1.5 bps/Hz, ensuring a baseline level of service quality for typical data applications such as web browsing, video, voice over internet protocol (VoIP), and IoT devices. Our method guarantees that all users meet the minimum rate requirement, resulting in maximum fairness and a Jain's fairness index of one [40]. It then calculates the optimal power allocation. Finally, the results are normalized to achieve fairness.

Note: We will use the term "Hybrid" to refer to hybrid JT-CoMP OMA/NOMA, "OMA" for pure CoMP OMA, "NOMA" for pure CoMP NOMA and " Non-CoMP NOMA" for fully non-CoMP NOMA in the plots and result discussions.

6.1. EE performance with varying SNR

6.1.1. General analysis

Fig. 3 depicts the EE performance of the proposed system. In general, the EE improves as the SNR increases across all configurations and power allocation schemes. The hybrid scheme performs better than all OMA, NOMA and non-CoMP NOMA schemes, regardless of the power allocation scheme used. With OPCOM, NOMA outperforms OMA until SNR = 10 dB. This is due to its effectiveness in utilizing non-orthogonal resource allocation, which enables the support of two user with different channel conditions. The improved EE of OMA in high SNR region is a result of the decreased effectiveness of NOMA caused by a rise in INUI among NOMA users. The proposed approach uses a hybrid strategy to dynamically switch between OMA and NOMA based on real-time factors such as channel conditions, SNR, CoMP and non-CoMP user pairings, and unpaired users. At an SNR of 3 dB, the hybrid scheme employing OPCOM demonstrates around 23% superior performance compared to NOMA, 53% compared to OMA and 121% compared to non-CoMP NOMA . The proposed solution shows a 35% improvement compared to the hybrid approach utilizing UPAM. At 7 dB, the performance gap slightly decreases. This decrease is due to the optimized method consuming less power, which is constrained by a constant minimum rate R^{min}, compared to a fixed power consumption of the UPAM approach at higher SNR levels.

It is generally observed that non-CoMP NOMA tends to have the lowest EE for both UPAM and OPCOM in comparison to other baseline techniques. ICI from neighboring SBSs is a significant issue in non-CoMP NOMA as each SBS operates independently, which in turn necessitates increased power consumption to meet the minimum rate requirements. On the other hand, the application of JT-CoMP to both OMA and NOMA coordinates transmissions among both SBSs to manage interference. Thus, this coordination turns potential interference into meaningful signal. The signal strength is enhanced significantly, resulting in a reduction in the transmission power needed. This, in turn, leads to improved EE and network performance.

6.1.2. Impact of SIC on EE performance

We evaluate our proposed model by analyzing the power consumption factor of SIC, allowing for a more practical comparison with the schemes under consideration. Fig. 4 demonstrates that the overall trends with all schemes are similar to Fig. 3, where SIC power consumption factor is not considered. However, the EE of the hybrid approach is reduced in this case, as compared to the one that does not consider SIC. Fig. 4 shows that with OPCOM, OMA outperforms NOMA at a lower SNR region than Fig. 3. This is because the SIC is exclusively used at

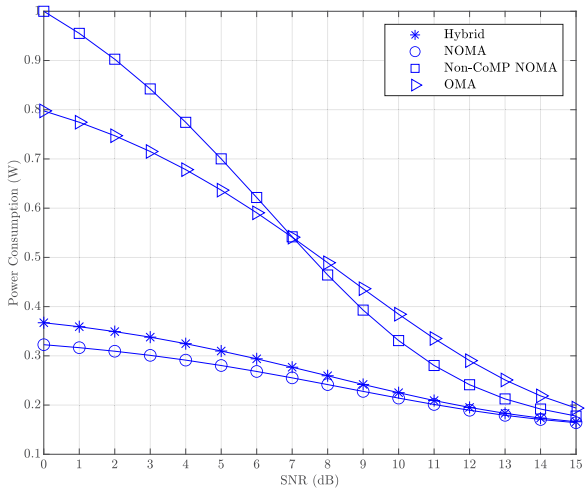

Fig. 5. Power consumption analysis of proposed algorithm with OPCOM without considering SIC power.

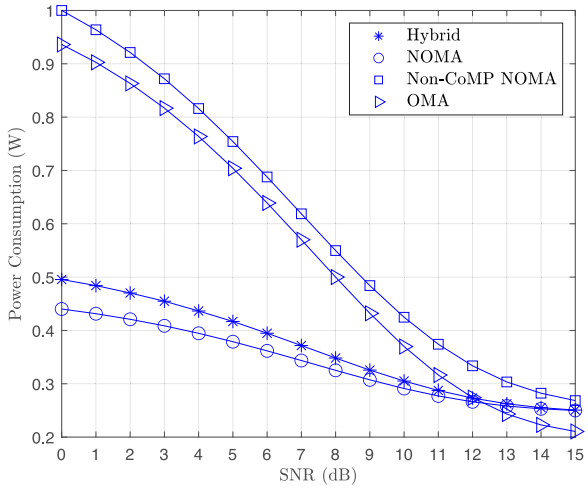

Fig. 6. Power consumption analysis of proposed algorithm with OPCOM considering SIC.

the near NOMA users, which has a negative impact in comparison to the simple OMA receivers. When taking power consumption of SIC into account non-CoMP NOMA tends to behave the same and has the lowest EE for both UPAM and OPCOM in comparison to rest of the techniques due to interference by neighboring SBS.

6.2. Power consumption with varying SNR

6.2.1. General analysis

A comparison of the power consumption of all multiple-access schemes employing OPCOM across varying SNR is depicted in Fig. 5. Power consumption decreases as SNR improves in all schemes. This behavior suggests that increased SNR levels improve the effectiveness of transmitted power. Overall, the proposed system consistently consumes less power than non-CoMP NOMA,OMA but more than NOMA. NOMA enables multiple SUEs to be allocated on the same RB, justifying its decrease in power consumption where as non-CoMP NOMA gets affected by interference. The gap between OMA, non-CoMP NOMA and proposed scheme gradually decreases, and at higher SNR values, all schemes converge to each other. This occurs because all schemes can minimize power consumption when the strong intended signals overpower noise and interference, leading to similar power consumption levels. In non-CoMP NOMA interference can still be introduced by

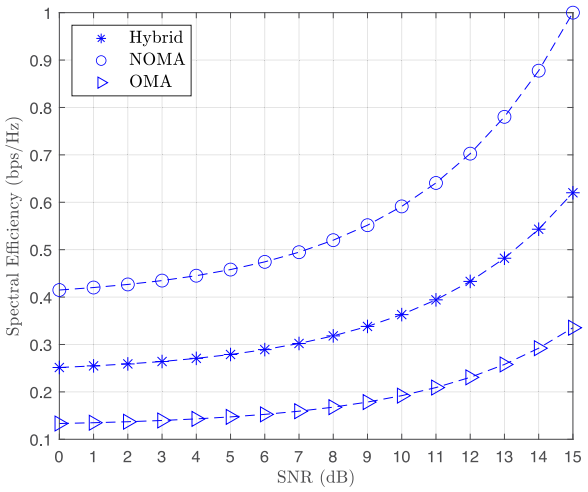

Fig. 7. Spectral efficiency of proposed algorithm with UPAM scheme.

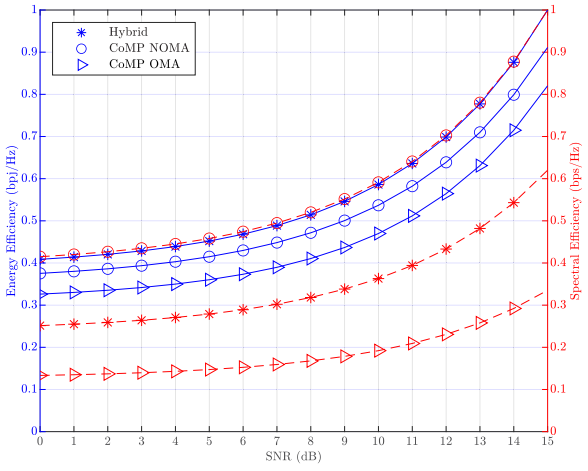

Fig. 8. Trade-off between spectral efficiency and energy efficiency of proposed algorithm with UPAM scheme.

neighboring SBS with high SNR. Nevertheless, the efficiency of NOMA in power allocation based on channel conditions enables it to enhance EE even at high SNR. This achieved by optimizing power levels for the two users, enhancing SE, and reducing power consumption.

6.2.2. Impact of SIC on power consumption

It is critical to consider the impact of SIC on power consumption because it is more realistic and can provide deeper insights. Fig. 6 shows an increase in overall power consumption for the proposed hybrid, non-CoMP NOMA and NOMA schemes compared to Fig. 5, whereas OMA is the same because OMA does not incorporate SIC. When the SNR is low, OMA and non-CoMP NOMA consume the most power, while hybrid and NOMA use approximately half as much. Since OMA allots dedicated resources to each user, power consumption may rise when SNR is low. Despite having slightly higher power consumption than NOMA at lower SNR levels, the hybrid approach outperforms OMA overall. At 4 dB, a 46% less power is consumed by proposed hybrid approach against OMA, a 55% less than non-CoMP NOMA, whereas 9% more power consumption when compared to NOMA. The hybrid approach gradually approaches NOMA in terms of power usage as SNR level increases. This implies that the hybrid approach moves towards the more power-efficient features of NOMA under favorable channel conditions. Therefore, adopting the hybrid approach is questionable if NOMA consumes less power and performs comparably to the proposed approach at higher SNR levels. Although the hybrid approach

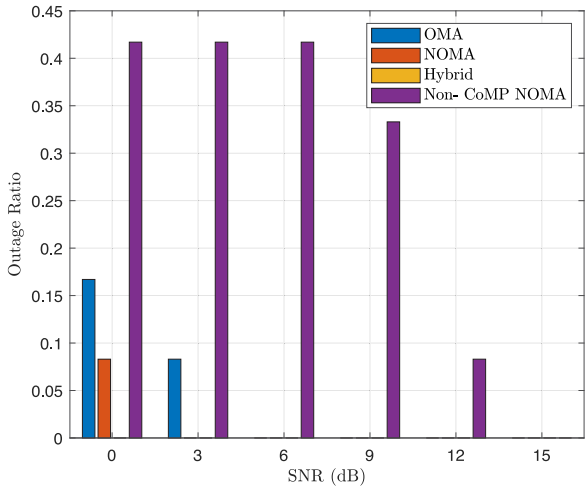

Fig. 9. Outage ratio vs SNR for $R^{min} = 1.5$ bps/Hz.

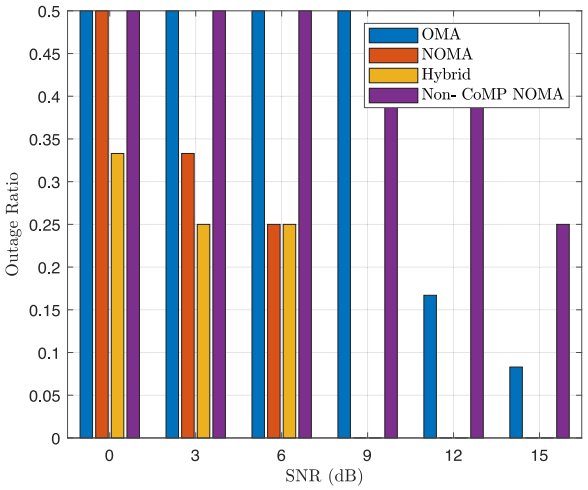

Fig. 10. Outage ratio vs SNR for $R^{min} = 3$ bps/Hz.

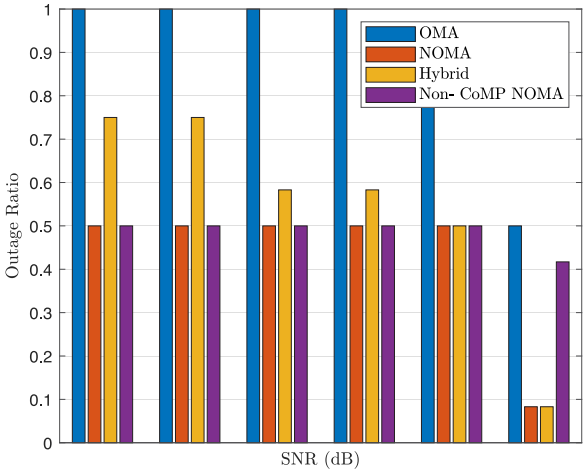

Fig. 11. Outage ratio vs SNR for $R^{min} = 5$ bps/Hz.

consumed 12% more power than NOMA at 0 dB, it improves EE by 26%, as shown in Fig. 4. The hybrid method outperforms NOMA at 5 dB, consumes only 9% more power, and is 30% more energy-efficient. Overall, the hybrid approach outperforms NOMA and OMA both.

6.3. Spectral efficiency with varying SNR

Since SE is the ratio of achieved data rate and the available/consumed bandwidth, we determined the optimal power value with respect to R^{min} in OPCOM. As a result, the numerator is consistent across all schemes and shows no significant pattern. Therefore, SE of OMA, NOMA, and hybrid schemes is evaluated with UPAM scheme. Fig. 7 shows that NOMA outperforms the other schemes in terms of SE. It clearly demonstrates its superiority when compared to the proposed hybrid approach and OMA. The hybrid scheme is approximately 27% less efficient than NOMA, but 99% more spectral efficient than OMA.

6.3.1. Spectral efficiency relationship with EE with varying SNR

SE is improved by dynamic power allocation based on users' channel conditions. In addition, it can improve EE since users with stronger channel gains require less power to achieve their desired data rates, resulting in reduced energy consumption across the network. In general, there is a trade-off between SE and EE where increasing SE requires higher transmission power, which could potentially decrease overall EE. However, in Fig. 8, both SE and EE are increasing, with EE showing a more rapid increase in hybrid and OMA schemes. SE increases logarithmically with SNR. EE improves more noticeably due to efficient power allocation and interference management. Nevertheless, the rate at which SE increases is generally lower than that of EE. At higher SNRs, the increased power mainly improves EE by reducing the amount of energy needed to transmit each bit. However, the improvements in SE become less significant as the relationship between SE and SNR follows a logarithmic pattern.

6.4. Outage analysis

The outage ratios of CoMP NOMA, CoMP OMA, hybrid CoMP OMA NOMA, and fully non-CoMP NOMA schemes are compared at various SNR values in Fig. 9, Fig. 10 and Fig. 11 for different values of R^{min}. All schemes demonstrate low outage ratios, with the hybrid scheme exhibiting the lowest among them, when considering $R^{min} = 1.5$ bps/Hz. The outage ratios show an increase across all schemes when R^{min} is set to 3 bps/Hz. However, the hybrid scheme is the most effective, particularly at higher SNR levels. At a R^{min} of 5 bps/Hz, the hybrid scheme exhibits the lowest outage ratio at high SNR levels, even though it initially has a higher ratio at lower SNR. When R^{min} requirements are increased, the hybrid approach starts to behave more like NOMA due to the power allocation strategies aligning to meet stringent rate demands. This results in similar power consumption patterns. In general lower SNR values result in higher outage ratios for all schemes. It is not unexpected that there are more frequent outages due to the poorer signal quality. Another important result from these figures can be drawn that hybrid and CoMP NOMA schemes outperform fully non-CoMP NOMA because edge users are cooperatively served by joint transmission of coordinating SBSs, thereby eliminating interference from neighboring SBSs. The CoMP transmission mitigates the interference by coordinating the joint transmission from SBSs, resulting in improved received SINR and data rate for users. This ultimately leads to a decrease in outages. Hybrid scheme consistently displays lowest outage ratio across all SNR levels and R^{min} values effectively demonstrating its superiority over rest of the baseline schemes.

6.5. Comparison of proposed heuristic with exhaustive search approach

To validate the performance of the proposed DCEAMA algorithm, we compare it to an exhaustive search method that considers user pairing and multiple-access selection by exhaustively pairing CoMP and non-CoMP users. Furthermore, we select either OMA or NOMA for each potential pairing to maximize the sum data rate. This systematic approach enables us to identify the most efficient multiple-access strategy for any possible situation. We then compute the EE of the network for each scenario to evaluate its overall performance. The scenario

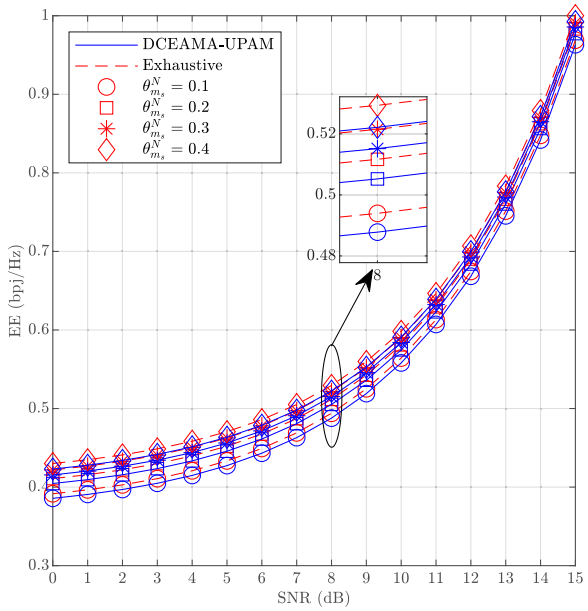

Fig. 12. Comparison of proposed heuristic with Exhaustive search algorithm.

with the highest EE is selected as the optimal case. As depicted in Fig. 12, the EE of our proposed heuristic is comparable to that of the exhaustive approach. On average, the exhaustive search is only approximately 1.35% more energy-efficient than the proposed approach. Our analysis primarily examines user pairing and multiple-access selection. To evaluate the performance of the proposed approach, we conduct a comparative analysis using four distinct power coefficients for near NOMA users, i.e., $\theta^N_{m_s} = \{0.1, 0.2, 0.3, 0.4\}$. This enables a comprehensive assessment of the approach's effectiveness by examining how varying power allocations impact performance. A larger $\theta^N_{m_s}$ value improves performance in terms of EE.

In terms of computational complexity, the heuristic performs better than the exhaustive search method. The computational complexity of heuristic is $O(S \cdot M_s + M_s \log M_s)$, whereas the complexity of exhaustive search is approximately $O\left(S \cdot M_s^2\right)$. The heuristic scales linearly with the number of SUEs and SBSs, whereas the complexity of exhaustive search increases exponentially with the number of users, leading to a higher number of unique pairings per user. This surge considers symmetry for each SBS, intensifying the computational demand. However, the exhaustive search method guarantees the best solution. Overall, the proposed DCEAMA method is computationally simpler and achieves nearly equivalent results.

7. Conclusion and future work

In this paper, we have investigated a novel non-coherent JT-CoMP enabled hybrid OMA/NOMA system for improving the EE of power-constrained IoT devices in B5G system. The proposed system is mathematically modeled as an MINLP optimization problem, which is solved by proposing a low complexity heuristic algorithm, termed as DCEAMA algorithm. The proposed algorithm involves several steps, including user categorization, CoMP/non-CoMP pairing, selecting optimal multiple-access scheme pairwise based on maximum sum data rate using UPAM, and finally evaluating the network EE to consume minimum power using OPCOM. Simulation results show that the proposed scheme outperforms traditional CoMP OMA and CoMP NOMA schemes in terms of EE across all SNR values. However, when considering the SIC power consumption factor for NOMA, the EE reduces compared to the basic model and is relatively less energy-efficient than pure CoMP OMA at high SNR values. In conclusion, our proposed hybrid approach combines the efficiency of NOMA and the reliability of OMA to provide a flexible solution. Switching between these strategies improves system performance by adjusting to real-time channel conditions. This approach achieves an effective combination of spectrum efficiency and interference reduction, catering to wide range of user requirements while also ensuring the system's adaptability to changing technological demands.

In the future, we plan to investigate the use of machine learning techniques, such as reinforcement learning (RL), to address this optimization problem. The RL agent can optimize EE by interacting with the hybrid multiple-access HetNet environment and intelligently choosing between NOMA and OMA. Further research can expand the user cluster and accommodate more CoMP users within a pair. The hybrid multi-access HetNet can be integrated into the smart city architecture to effectively handle transmission and provide seamless connectivity to users (or devices in smart cities), considering the diverse nature and locations of the traffic generated in smart cities. This integration will help cater to the different quality of service requirements of HetNets in different environments. Furthermore, this research may be extended to the concept of moving small cells for in-vehicle mobile users that have varying data load, uninterrupted services and enhanced QoS requirements.

CRediT authorship contribution statement

Aamina Akbar: Writing – original draft, Resources, Methodology, Conceptualization. **Ashfaq Ahmed:** Writing – review & editing, Methodology. **Adnan Zafar:** Supervision. **Sobia Jangsher:** Writing – review & editing, Supervision, Investigation.

Declaration of competing interest

The authors declare that they have no known competing financial interests or personal relationships that could have appeared to influence the work reported in this paper.

Data availability

No data was used for the research described in the article.

Declaration of Generative AI and AI-assisted technologies in the writing process

During the preparation of this work the authors used ChatGPT in order to enhancing the manuscript's writing quality and correcting spelling and grammatical errors. After using this tool/service, the authors reviewed and edited the content as needed and takes full responsibility for the content of the publication.

References

[1] B.S. Khan, S. Jangsher, A. Ahmed, A. Al-Dweik, URLLC and eMBB in 5G industrial IoT: A survey, IEEE Open J. Commun. Soc. 3 (2022) 1134–1163, http://dx.doi.org/10.1109/OJCOMS.2022.3189013.

[2] S. Jangsher, V.O.K. Li, Resource allocation in moving small cell network, IEEE Trans. Wireless Commun. 15 (7) (2016) 4559–4570, http://dx.doi.org/10.1109/TWC.2016.2542246.

[3] H.J. Damsgaard, A. Ometov, M.M. Mowla, A. Flizikowski, J. Nurmi, Approximate computing in B5G and 6G wireless systems: A survey and future outlook, Comput. Netw. (2023) 109872.

[4] Y. Liu, W. Yi, Z. Ding, X. Liu, O.A. Dobre, N. Al-Dhahir, Developing NOMA to next generation multiple access: Future vision and research opportunities, IEEE Wireless Commun. 29 (6) (2022) 120–127, http://dx.doi.org/10.1109/MWC.007.2100553.

[5] A. Ahmed, A. Al-Dweik, Y. Iraqi, E. Damiani, Integrated terrestrial-wired and LEO satellite with offline bidirectional cooperation for 6G IoT networks, IEEE Internet Things J. (2024) 1, http://dx.doi.org/10.1109/JIOT.2023.3349144.

[6] R. Tanbourgi, S. Singh, J.G. Andrews, F.K. Jondral, Analysis of non-coherent joint-transmission cooperation in heterogeneous cellular networks, in: IEEE Intl. Conf. Commun., ICC, 2014, pp. 5160–5165.

[7] M.S. Ali, E. Hossain, D.I. Kim, Coordinated multipoint transmission in downlink multi-cell NOMA systems: Models and spectral efficiency performance, IEEE Wireless Commun. 25 (2) (2018) 24–31.

[8] H. Tabassum, M.S. Ali, E. Hossain, M.J. Hossain, D.I. Kim, Uplink vs. downlink NOMA in cellular networks: Challenges and research directions, in: IEEE 85th Veh. Technol. Conf. (VTC Spring), 2017, pp. 1–7.
[9] Z. Ding, Y. Liu, J. Choi, Q. Sun, M. Elkashlan, I. Chih-Lin, H.V. Poor, Application of non-orthogonal multiple access in LTE and 5G networks, IEEE Commun. Mag. 55 (2) (2017) 185–191.
[10] A. Akbar, S. Jangsher, F.A. Bhatti, NOMA and 5G emerging technologies: A survey on issues and solution techniques, Comput. Netw. 190 (2021) 107950.
[11] M. Khalid, A. Akbar, H.K. Qureshi, S. Jangsher, Joint backhaul pairing and resource allocation of moving small cells using NOMA, in: Intl. Symp. on Netw., Comput. and Commun., ISNCC, 2023, pp. 1–6.
[12] H. Yahya, A. Ahmed, E. Alsusa, A. Al-Dweik, Z. Ding, Error rate analysis of NOMA: Principles, survey and future directions, IEEE Open J. Commun. Soc. 4 (2023) 1682–1727.
[13] Z. Liu, G. Hou, Y. Yuan, K.Y. Chan, K. Ma, X. Guan, Robust resource allocation in two-tier NOMA heterogeneous networks toward 5G, Comput. Netw. 176 (2020) 107299.
[14] Y. Wu, J. Zhu, X. Chen, Y. Zhang, Y. Shi, Y. Xie, QoS-based resource allocation for uplink NOMA networks, Comput. Netw. 238 (2024) 110084.
[15] M. Vaezi, R. Schober, Z. Ding, H.V. Poor, Non-orthogonal multiple access: Common myths and critical questions, IEEE Wireless Commun. 26 (5) (2019) 174–180.
[16] Y. Sun, Z. Ding, X. Dai, O.A. Dobre, On the performance of network NOMA in uplink CoMP systems: A stochastic geometry approach, IEEE Trans. Commun. 67 (7) (2019) 5084–5098.
[17] Z. Liu, G. Kang, L. Lei, N. Zhang, S. Zhang, Power allocation for energy efficiency maximization in downlink CoMP systems with NOMA, in: IEEE Wireless Commun. Netw. Conf., WCNC, 2017, pp. 1–6.
[18] A.J. Muhammed, Z. Ma, Z. Ding, M. Xiao, P. Fan, W. Xu, G. Liu, Z. Zhang, Resource allocation for energy-efficient NOMA system in coordinated multi-point networks, IEEE Trans. Veh. Technol. 70 (2) (2021) 1577–1591.
[19] Y. Al-Eryani, E. Hossain, D.I. Kim, Generalized coordinated multipoint (GCoMP)-enabled NOMA: Outage, capacity, and power allocation, IEEE Trans. Commun. 67 (11) (2019) 7923–7936.
[20] A. Kilzi, J. Farah, C.A. Nour, C. Douillard, Mutual successive interference cancellation strategies in NOMA for enhancing the spectral efficiency of CoMP systems, IEEE Trans. Commun. 68 (2) (2019) 1213–1226.
[21] H. Shao, H. Zhang, L. Sun, Y. Qian, Resource allocation and hybrid OMA/NOMA mode selection for non-coherent joint transmission, IEEE Trans. Wireless Commun. (2021).
[22] C.-H. Liu, D.-C. Liang, Heterogeneous networks with power-domain NOMA: Coverage, throughput, and power allocation analysis, IEEE Trans. Wireless Commun. 17 (5) (2018) 3524–3539.
[23] M.S. Ali, E. Hossain, A. Al-Dweik, D.I. Kim, Downlink power allocation for CoMP-NOMA in multi-cell networks, IEEE Trans. Commun. 66 (9) (2018) 3982–3998.
[24] M. Moltafet, R. Joda, N. Mokari, M.R. Sabagh, M. Zorzi, Joint access and fronthaul radio resource allocation in PD-NOMA-based 5G networks enabling dual connectivity and CoMP, IEEE Trans. Commun. 66 (12) (2018) 6463–6477.
[25] M. Elhattab, M.-A. Arfaoui, C. Assi, CoMP transmission in downlink NOMA-based heterogeneous cloud radio access networks, IEEE Trans. Commun. 68 (12) (2020) 7779–7794.
[26] D.K. Hendraningrat, M.B. Shahab, S.Y. Shin, Virtual user pairing non-orthogonal multiple access in downlink coordinated multipoint transmission, 2019, arXiv preprint arXiv:1903.10674.
[27] Z.-X. Huang, Y.C. Peng, Y.-C. Lo, J.-C. Kao, H.-H. Su, Resource allocation for non-orthogonal multiple access with coordinated multipoint support, in: IEEE 91st Veh. Technol. Conf., VTC2020-Spring, 2020, pp. 1–5.
[28] A. Ebrahim, A. Celik, E. Alsusa, M.W. Baidas, A. Eltawil, Hybrid multiple-access: Mode selection, user pairing and resource allocation, IEEE Access (2023).
[29] J. Shi, W. Yu, Q. Ni, W. Liang, Z. Li, P. Xiao, Energy efficient resource allocation in hybrid non-orthogonal multiple access systems, IEEE Trans. Commun. 67 (5) (2019) 3496–3511.
[30] F. Tanaka, H. Suganuma, F. Maehara, Hybrid multiple access scheme using NOMA and OMA simultaneously considering user request, in: Intl. Symp. Wireless Pers. Multimedia Commun., WPMC, 2021, pp. 1–5.
[31] A.S. Marcano, H.L. Christiansen, A novel method for improving the capacity in 5G mobile networks combining NOMA and OMA, in: IEEE 85th Veh. Technol. Conf., (VTC Spring), 2017, pp. 1–5.
[32] U. Ghafoor, H.Z. Khan, M. Ali, A.M. Siddiqui, M. Naeem, I. Rashid, Energy efficient resource allocation for H-NOMA assisted B5G HetNets, IEEE Access 10 (2022) 91699–91711.
[33] A. Jee, K. Janghel, S. Prakriya, Performance of adaptive multi-user underlay NOMA transmission with simple user selection, IEEE Trans. on Cognitive Commun. Netw. 8 (2) (2022) 871–887.
[34] A. Jee, S. Prakriya, Performance of a NOMA/OMA scheme with novel power control and mode selection, in: Intl. Conf. Commun., ICC, IEEE, 2023, pp. 6138–6144.
[35] Performance of underlay cooperative hybrid OMA/NOMA scheme with user selection.
[36] S.R. Magalhaes, S. Bayhan, G. Heijenk, Impact of power consumption models on the energy efficiency of downlink NOMA systems, IEEE Trans. Green Commun. Netw. (2023).
[37] A.J. Muhammed, Z. Ma, Z. Ding, M. Xiao, P. Fan, W. Xu, G. Liu, Z. Zhang, Resource allocation for energy-efficient NOMA system in coordinated multi-point networks, IEEE Trans. on Veh. Technol. 70 (2) (2021) 1577–1591.
[38] M.S. Ali, H. Tabassum, E. Hossain, Dynamic user clustering and power allocation for uplink and downlink non-orthogonal multiple access (NOMA) systems, IEEE Access 4 (2016) 6325–6343.
[39] F. Fang, J. Cheng, Z. Ding, Joint energy efficient subchannel and power optimization for a downlink NOMA heterogeneous network, IEEE Trans. Veh. Technol. 68 (2) (2018) 1351–1364.
[40] R.K. Jain, D.-M.W. Chiu, W.R. Hawe, et al., A quantitative measure of fairness and discrimination, vol. 21, Eastern Research Laboratory, Digital Equipment Corporation, Hudson, MA, 1984, p. 1.

Aamina Akbar is currently enrolled in the Doctoral Program of the Institute of Space Technology (IST), Pakistan, to pursue PhD studies in Electrical Engineering with a specialization in Wireless Communication under the prestigious HEC Faculty Development Scholarship Program (Indigenous program). She has done her B.E. Electrical (Telecom) Engineering from the National University of Science and Technology (NUST), Pakistan, and her MS Electrical (Telecom) Engineering from the Center of Advanced Studies in Engineering (CASE), Pakistan, in 2010 and 2014, respectively. She is a lecturer in the department of engineering and IT at the Foundation University School of Science and Technology (FUSST), Pakistan, for 10 years.

Dr. Ashfaq Ahmed (Senior Member, IEEE) received the M.S. and Ph.D. Degree from the Department of Electronics and Telecommunications, Politecnico di Torino, Torino, Italy, in 2010 and 2014, respectively. He is currently affiliated with the center for cyber–physical systems (C2PS), Department of Computer & Communication Engineering, Khalifa University (KU), Abu Dhabi, UAE. He worked as an Assistant Professor at the Department of Electrical & Computer Engineering, COMSATS University Islamabad, Wah campus, Pakistan from March 2014 to March 2021. His research interests include hardware security, security protocols, computational intelligence, evolutionary algorithms, convex optimization, resource allocation, and applied optimization for 5G and beyond 5G applications, cloud computing,and physical layer wireless communication. He has hands-on experience with simulation and modeling of optimization problems, as well as working with a variety of optimization toolboxes, including the MATLAB optimization toolbox and the OPTI toolbox. He also developed heuristics and applied several meta-heuristics to various optimization problems.

Adnan Zafar received his B.S. degree in Communication Systems Engineering from the Institute of Space Technology (IST), Islamabad, Pakistan, in 2007. He then received his M.Sc. degree (Distinction) in Satellite Communications Engineering and a Ph.D. degree in Electronic Engineering both from the University of Surrey, Guildford, UK in 2011 and 2018, respectively. He has also worked as a Research Assistant at the Institute for Communication Systems, home of 5G Innovation Centre (5GIC), University of Surrey, UK. He is currently working as Head of the Electrical Engineering Department at IST, Pakistan. His research interests broadly lie in Signal Processing for Wireless Communication.

Sobia Jangsher received the B.E. degree in electronics engineering and the M.S. degree in communication system engineering from the National University of Science and Technology, Pakistan, and the Ph.D. degree in wireless communication from The University of Hong Kong, Hong Kong. From November 2015 to January 2021, she was working as an Assistant Professor with the Institute of Space Technology, Islamabad, Pakistan. She was associated with Khalifa University from January 2020–February 2023. She has also worked as senior researcher in wireless communication lab in Tyndall National Institute for 6 months. She is currently working as an Assistant Professor in School of Electronic Engineering in Dublin City University, Ireland. Her research interests include optimization/resource allocation for 5G/6G communication systems and machine learning for wireless communication.